GIANT SOLAR ARCHES AND CORONAL MASS EJECTIONS IN NOVEMBER 1980

ZDENĚK F. ŠVESTKA

Laboratory for Space Research, SRON, The Netherlands

and

University of California at San Diego, La Jolla, CA, U.S.A.

BERNARD V. JACKSON

University of California at San Diego, La Jolla, CA, U.S.A.

RUSSELL A. HOWARD and NEIL R. SHEELEY, JR.

E.O. Hulburt Center for Space Research,
US Naval Research Laboratory, Washington, D.C., U.S.A.

(Received 30 November, 1988; in revised form 23 January, 1989)

Abstract. Using data from the SOLWIND coronagraph and photometers aboard HELIOS-A we examine coronal mass ejections from an active region which produced a series of giant post-flare coronal arches. HXIS X-ray observations reveal that in several cases underlying flares did not disrupt these arch structures, but simply revived them, enhancing their temperature, density and brightness. Thus we are curious to know how these quasi-stationary X-ray structures could survive in the corona in spite of recurrent appearances of powerful dynamic flares below them. We have found reliable evidence that two dynamic flares which clearly revived the preexisting giant arch were not associated with any mass ejection. After two other flares, which were associated with mass ejections, the arch might have been newly formed when the ejection was over. In one of these cases, however, the arch had typical characteristics of a revived structure so that it is likely that it survived a powerful mass ejection nearby. In a magnetic configuration of the arch which results from potential-field modelling (Figure 1(b)) such a survival seems possible.

1. Introduction

A series of five dynamic (two-ribbon) flares occurred in AR 2779 on 5–7 November, 1980 and at least four of them were followed by brightenings of extensive coronal structures seen by the Hard X-Ray Imaging Spectrometer (HXIS; Van Beek *et al.*, 1980) on board the SMM in >3.5 keV X-rays (Švestka, 1984; Fárník, van Beek, and Švestka, 1986). In analogy with the earlier event of 21 May, 1980 (Švestka *et al.*, 1982a) these structures have been interpreted as giant coronal arches extending above the active region and seen in X-rays up to altitudes beyond 150 Mm. Table I summarizes the observations of AR 2779 on 5–9 November, 1980. The best HXIS data have been obtained on the arch No. 2 which could be observed (intermittently) in X-rays from its beginning close to 15 UT on 6 November through its whole development until 05 UT the next day when the arch No. 3 began to appear.

Since the discovery of the giant arches by HXIS we have been puzzled by the problem of how the same active region can produce both mass ejections and quasi-stationary long-lived structures in the solar corona; at least in some cases both these phenomena

Solar Physics **122** (1989) 131–143.

TABLE I

Chronological summary of ground-based, SOLWIND, HELIOS-A, and HXIS observations

Date Nov.	Time (UT)	Dynamic flare	SOLWIND (2.6–8.0 R_0)	HELIOS-A (>40 R_0)	HXIS
4			Corona above AR enhanced; no transient	*No data*	*Pointed elsewhere*
5	13 : 35		*Last observation*		
	13 : 55	X-ray max. X4/E78/II + IV	*No data*		
	20 : 57		*First observation* Very bright coronal condensation with slow or no motion		
6	00 : 47		*Last observation*		
	03 : 52	X-ray max. X9/E70/II + IV	*No data*		
	06 : 24				*Repointed to AR* Giant arch No. 1 near maximum
	08 : 09		*First observation* Very weak remant of bright condensation disappearing		Arch No. 1 decaying in brightness
	09 : 36			*Switched on; first image* Enhancement seen behind the Sun	
	11 : 55		*Last observation*		
	15 : 26	X-ray max. X1/E65/IV	*No data*		Revival of the preceding arch: giant arch No. 2
	17 : 17			New CME to the south added to the preceding enhancement	Maximum brightness of arch No. 2
	19 : 22		*First observation* faint remnants, no enhancement		Arch No. 2 decaying in brightness
7	02 : 24		*Last observation*		
	02 : 56			CME decaying	
	04 : 58	X-ray max. M3/E56	*No data*		Revival of the preceding arch: giant arch No. 3
	06 : 33		*First observation* No enhancement		Maximum brightness of arch No. 3

Table I (continued)

Date Nov.	Time (UT)	Dynamic flare	SOLWIND (2.6–8.0 R_0)	HELIOS-A (>40 R_0)	HXIS
7	10 : 11			CME decaying	Arch No. 3 decaying
	12 : 00		*Last observation*		Arch No. 3 decayed
	18 : 00		*No data*	CME decaying	
	20 : 58		*First observation* No enhancement		
	21 : 50	X-ray max. M2/E46			Appearance of giant arch No. 4
8	00 : 30				Maximum brightness of arch No. 4
	03 : 20		CME towards south at high latitude		
	04 : 00		*Last observation*		
	04 : 51			CME decayed	
	08 : 09		*First observation* No enhancement		
	10 : 44			Indicated onset of another CME	
	13 : 37		*Last observation*		Arch No. 4 decayed
	17 : 47		*First observation* No enhancement		
	19 : 17			New CME clearly developed	
9	05 : 46			CME decaying	Quite different structures developed
	11 : 38			CME decaying	
	13 : 27		*Last observation*		

seemed to be associated with the same flare event. In the case of the post-flare arch of 21 May, 1980 the mass ejection was an anomalous phenomenon, associated with a spray directed some 40 deg aside of the extension of the arch, while the dark filament in the active region did not erupt (McCabe *et al.*, 1986). The mass ejections on 5–7 November have not been studied in detail so far and we intend to do so in this paper.

The final impulse for this study was the discovery of chromospheric footpoints of the arch structure on 6–7 November in Hα images taken at Big Bear and in Udaipur (Martin, Švestka, and Bhatnagar, 1989, further referred to as paper MS&B). First we knew only the eastern set of the footpoints, marked as a black plage in Figure 1. The Hα brightness variations of this plage correlated closely with the X-ray variations of the arches (cf. MS&B; complete observations are available only for the arch No. 2, but

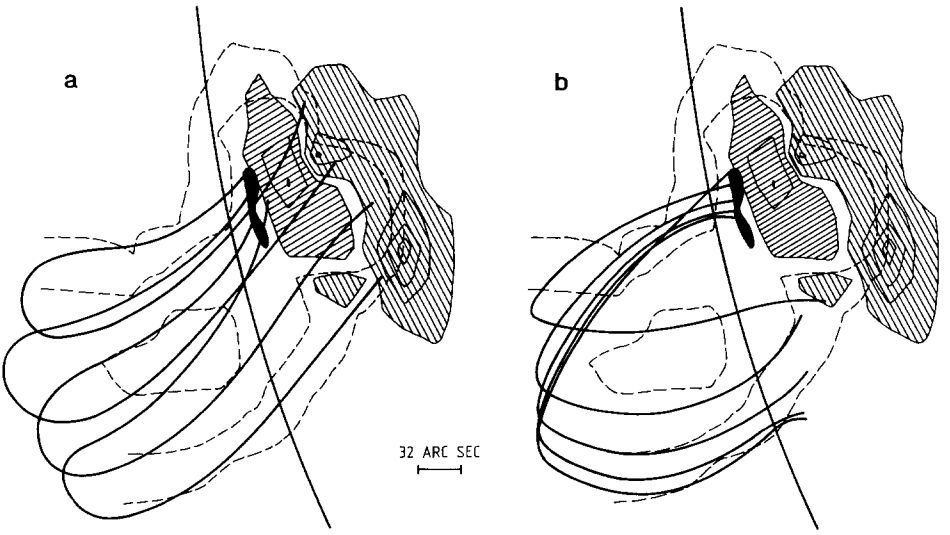

Fig. 1. Schematic drawings of the supposed magnetic structure of the post-flare coronal arches on 6 November, 1980. The active region magnetic field (as simplified by Kopp and Poletto, 1988) is shown by contours with opposite shading. Dashed lines extending over the eastern solar limb show the X-ray contours of the arch at 09 : 53 UT (after Švestka *et al.*, 1982b). Full lines are the supposed magnetic field lines in the arch. Originally only the north–east set of footpoints (the black plage) was known from Hα data. The second set of footpoints was assumed to be at the opposite side of the $H_{\parallel} = 0$ line in the active region, where many intermittent Hα brightenings occurred throughout the day (structure (a)). However, recent magnetic modelling by Kopp and Poletto (1988) places the second set of footpoints more to the south, out of the active region (structure (b)). (After MS&B.)

shorter periods of data for other three arches in the series confirm the reality of this footpoint). The location of the corresponding footpoints on the west side remained ambiguous. Because, during the existence of the arches, there were many intermittent brightenings along the $H_{\parallel} = 0$ line in the western part of the active region, we supposed that the unknown second set of footpoints was located along those positions, as indicated in Figure 1(a). Under this assumption, namely that the arch field lines crossed the $H_{\parallel} = 0$ line inside the active region, the arch seemed to have created some sort of magnetic ceiling which would make any existence of mass ejections from this active region essentially impossible (Figure 1(a)).

Quite recently this picture has changed. Kopp and Poletto (1988) used Kitt Peak magnetograms to model potential field lines rooted in the known set of the Hα footpoints, and found the second set of footpoints rather far from the active region, towards the south (Figure 1(b)). Though the potential approximation might oversimplify the situation and show only a part of the total set of fieldlines, Hα observations subsequently confirmed that there were Hα brightenings near the positions predicted by Kopp and Poletto, correlating in time with the occurrence of X-ray arches (cf. MS&B). Thus, at least some field lines of the arch, if not all of them, were rooted in the peripheral positions shown in Figure 1(b).

This implies that it appears possible now that mass ejections from the region might

be accomplished without destroying the whole quasi-stationary arch structure; but the longevity and persistence of this structure still remains peculiar if coronal mass ejections repeatedly accompanied the flares. (The last X-ray arch was seen as late as from 22 UT on 7 November to 12 UT on 8 November, cf. Fárník, van Beek, and Švestka, 1986).

The easiest explanation for the presence of both a mass ejection and a quasi-stationary arch assumes that the arch structure formed only after the coronal transient got detached and magnetically separated from the lower-lying magnetic field. But this is not what happened here. Both at 15 UT on 6 November (arch No. 2 in Table I) and at 05 UT on 7 November (arch No. 3) the preceding arch definitely did not disappear: the old arch was still clearly visible in >3.5 keV X-rays when the new arch began to brighten (cf. Švestka, 1984; and Hick and Švestka, 1987). This is the reason why we speak here about 'arch revivals'.

It is possible, as Table I shows, that also the arch No. 1, initiated by the flare at 03 : 52 UT on 6 November was a revival, because another major dynamic flare occurred in the same region 14 hours prior to it. It shows indeed some characteristics very similar to the revived arch No. 2, e.g., a slow rise of the brightness and temperature maximum through the arch which, after Hick and Švestka (1987), should characterize an arch revival. Thus, if there were any mass ejections, they must have left the quasi-stationary structures unaffected at least in the case of the arches 1 and 2, and probably also in the case of the structure preceding the arch 1. As we mentioned before, even late on 7 November and early on 8 November the arch still showed a similar shape and similar properties.

Therefore, the conclusion is that in most (or all) cases on 6 and 7 November the arch structure did not disrupt, but simply revived in temperature, density, and brightness when a new dynamic flare appeared in the active region below it. Let us check what was observed during the same period of time in the high corona (SOLWIND data) and in the nearby interplanetary space (HELIOS observations).

2. SOLWIND Observations

As of 4 November, 1980, SOLWIND, on board the P78–1 satellite, observed enhanced coronal brightness above the AR 2779 on the eastern limb (Figure 2(a)). The brightness increased only slightly during the day of 5 November until 13 : 35 UT. As Table I shows, the next picture of the corona was taken seven hours later, at 20 : 57 UT. By that time, the coronal condensation had brightened above the active region. This coronal enhancement is shown in Figure 2(b). It showed only very slow upward motion, if any, and stayed bright until at least 00 : 47 UT on 6 November, when this series of SOLWIND observations ended (Figure 2(c)). By 08 : 09 UT on 6 November, when the next image was obtained, the coronal feature had faded considerably as shown in Figure 2(d).

Because the only other important active region was near the central meridian, the coronal enhancement in Figure 2 was clearly associated with AR 2779. It might have been just an active region brightening as the region grew, but the more likely inter-

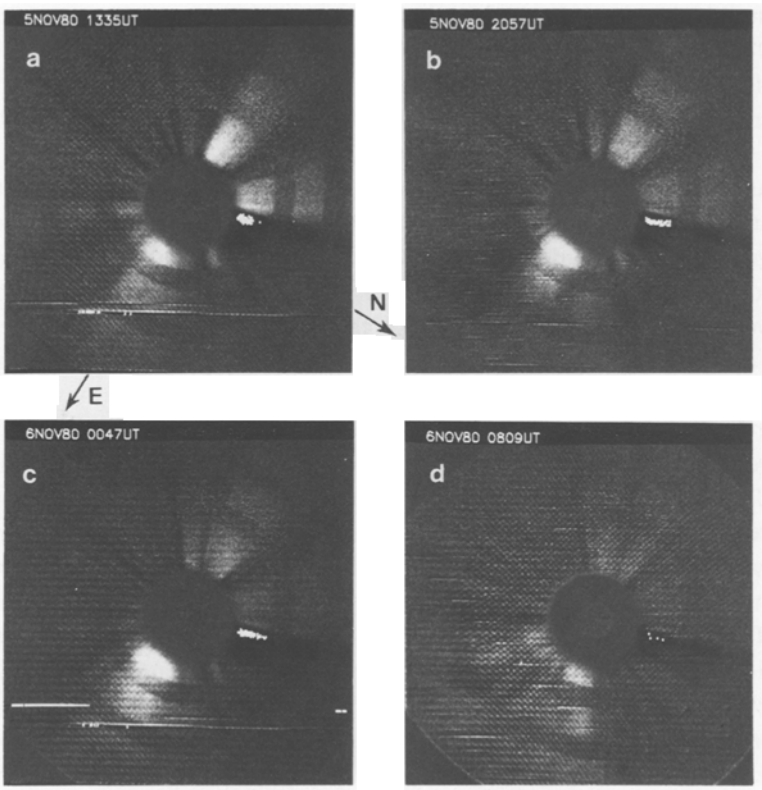

Fig. 2. SOLWIND difference images, substracted from a reference frame obtained during a quiet interval on 6 November well after the event. Note that we have used the unconventional reverse parity of the images with east to the right of north, because it looks that way in the sky. (a) 5 November 13 : 35 UT: enhanced corona above AR 2779; (b) 5 November 20 : 57 UT: very bright coronal condensation above AR 2779; (c) 6 November 00 : 47 UT: very little change in the shape and brightness of this structure; (d) 6 November 08 : 09 UT: the condensation has essentially disappeared.

pretation is that the enhancement followed the dynamic flare at 13 : 55 UT on 5 November which started just a few minutes after the image in Figure 2(a) was made. We have no evidence that this flare also produced a giant X-ray arch, because HXIS did not observe this region at that time (cf. Table I). Tentatively it has been assumed that this flare created the first arch in the series of subsequent revivals (Švestka, 1984). In any case, there is no reason why this flare could not be associated with a mass ejection. The flare produced radio bursts of types II and IV and such flares often are accompanied by coronal transients (Sheeley *et al.*, 1984; Robinson, 1986).

If so, however, the transient looks rather anomalous. Images of the corona obtained seven and eleven hours after this event (Figure 2(b) and 2(c)) show an unusual transient which was almost stationary, just a cloud of trapped electrons hanging above the active region. This bright cloud was seen as late as 00 : 47 UT on 6 November at an altitude of 3 to 6 solar radii so that it could not rise with higher mean speed than 60 km s^{-1}.

Moreover, its position at 00 : 47 UT (Figure 2(c)) seems to be essentially the same as three hours before (Figure 2(b)). Thus either the mass ejection was extremely slow, which is unlikely when type II/IV occurs, or the real mass ejection had been accomplished earlier and we see here a bright electron cloud left behind the detached ejected plasma.

One is tempted to suggest that in the latter case we see here the top of a giant coronal arch, similar to the structures which HXIS observed later on in X-rays. However, if this really is the same structure which HXIS observed, the difference in altitude is enormous: whereas the following HXIS arches were seen below 200 Mm, this tentative SOLWIND arch must have greatly exceeded 3 solar radii, i.e., an altitude of 1400 Mm.

According to Karpen and Howard (1987), at 3 R_0 (i.e., at an altitude of two solar radii above the solar surface) the minimum number of electrons per cm^2 along the line-of-sight needed to produce recognizable enhanced emission in SOLWIND images is $n_e s = 10^{16}$ cm^{-2}. With $s = 10^5$ km as the minimum lateral extent of the mass ejection one gets the maximum value of the required electron density: $n_e = 10^6$ cm^{-3}. This is a density which could be expected in the arch; even in the much weaker X-ray arch of 21 May, 1980 the density extrapolated from Culgoora radio observations exceeded 2×10^6 cm^{-3} at this altitude (cf. Švestka *et al.*, 1982a, Table I). Then, of course, another question can be immediately raised: why don't we see the other arches of 6 November in SOLWIND images as well?

The next SOLWIND picture was obtained at 08 : 09 UT, and the coronal condensation was then practically gone (Figure 2(d)), Remnants of any enhancement were further decreasing and from 11 : 21 UT onwards no enhanced coronal emission could be detected above the southern hemisphere until 03 : 20 UT on 8 November. This event, however, was a high-latitude ejection over the south pole which hardly could come from AR 2779 at 12° south. (See next section for a more extensive discussion of this event.) Thus, according to SOLWIND data, there is no evidence for any mass ejection associated with the flares that revived the arches Nos. 2 and 3, and there is also no coronal brightening associated with the giant arches seen in X-rays.

However, the densities of these arches at 3 R_0 should definitely exceed the limit of 10^6 cm^{-3} since they were by an order of magnitude more intense in X-rays than the arch of 21 May, 1980 which we used for the comparison above. (Note that 3×10^5 cm^{-3} is the density of the ambient corona at that altitude.) Thus, the absence of any coronal emission in SOLWIND images later on 6 November needs an explanation, and there are five possibilities to be discussed:

(1) The density limit given by Karpen and Howard (1987) is underestimated.

This really may be the case. Their estimate was based on a minimum mass of 1×10^{-8} g cm^{-2}, whereas Jackson, Rompolt, and Švestka (1987) found a minimum mass of 2×10^{-8} g cm^{-2} between 5 and 6 R_0, where the estimate has the highest accuracy. From the graph shown by Karpen and Howard (their Figure 1) the noise level is four times worse at 3 R_0 than at 5–6 R_0. Thus the minimum mass which produces recognizable emission at 3 R_0 should be 8×10^{-8} g cm^{-2} which enhances the minimum density to 8×10^6 cm^{-3}.

Another source of underestimation may be the size of the studied area. Karpen and Howard considered 3 × 3 pixels (about 0.5 R_0 on a side) to determine their noise level. Thus the noise levels they find are from a far larger average coronal area than for the single pixels that were used in Skylab data with which they make a comparison. The noise level that is determined is a 2σ level instead of 3σ level, more appropriate for a detection of small features which may appear in only one pixel. It is difficult to estimate quantitatively the impact of these effects, but it seems quite clear that the minimum mass at 3 R_0 could be raised to 10^{-7} g cm^{-2} as the lower limit. With $s = 10^5$ km, as above, one finds then the density $n_e = 10^7$ cm^{-3}, but this density value depends on the real extent of the mass-ejection along the line-of-sight and on its fine structure.

(2) The arch has a structure of separated discrete loops (HXIS observed the X-ray arches with a poor angular resolution of 32 arc sec) so that one has to take into account a very small filling factor.

However, as a matter of fact, the value of $s = 10^5$ km that we have used already implies a filling factor of 0.2 or less, because the real extension along the line of sight very probably exceeded 1 R_0 (assuming the extent along the line-of-sight comparable to the latitudinal extension of the electron cloud seen in Figures 2(b) and 2(c)). It is unlikely that much lower filling factors could be used.

(3) As the active region was carried westward onto the solar disk the SOLWIND coronagraph would have been less able to see the giant arches.

First, the coronagraph has a decreased sensitivity to light scattered from out of the sky plane, but this effect cannot reduce the brightness by more than 50%. Second, a feature of a given height, say 3 R_0, would be increasingly occulted as it rotates onto the disk. The position of the active region at 20 : 57 UT on 5 November (Figure 2(b)) was 74° east of central meridian. Hence, the projected distance of 3.0 R_0 corresponded to radial altitude of 3.12 R_0. At 08 : 09 UT on 6 November (Figure 2(d)) the active region was at 68° east, hence, this structure at 3.12 R_0 altitude should be projected at an apparent distance of 2.89 R_0. Clearly, at least the arch No. 1 should be visible in SOLWIND images above the occulting disk.

(4) The arches were so very much inclined from the radial direction that the projected distance of 3 R_0 actually corresponds to much higher altitudes and thus lower densities.

In order to check upon it, we have asked G. Poletto to calculate the inclination of magnetic field lines that form the arch in her magnetic modelling (Kopp and Poletto, 1988). She has found (private communication) that the field line inclination was within 16° and 30° towards east with respect to the radial plane. This implies that the inclination actually compensates for the effect of solar rotation.

(5) The arches are structures confined to the corona below 1.5 R_0, as we see them in X-rays, so that our extrapolation of the density toward higher altitudes is incorrect.

In the case of the arch of 21 May, 1980 the density estimates were modelled from radio images (cf. Figures 6 and 9, and Table I in Švestka *et al.*, 1982a), but for the November series of arches we have no suitable unrefracted metric radio images to use for such a modelling.

Thus the summary of this discussion is as follows:

The fact that the SOLWIND coronagraph did not see the giant arches No. 1 and 2 on 6 November implies two possibilities: either those arches had much lower density than the preceding arch on 5 November tentatively imaged in Figures 2(b) and 2(c) (with the sensitivity limit of the SOLWIND coronagraph overestimated by at least an order of magnitude (cf. item (1) above); or the coronagraph did not see any giant arches. Assuming that the arches were of comparable intensity, temperature, and density (as the arches No. 1 and 2 seem to be, cf. Švestka, 1984), one has to conclude that the coronal feature in Figures 2(b) and 2(c) was not the top of a giant arch, but another kind of a stationary or very slowly moving coronal condensation above the active region.

The impact of the flare at 03 : 52 UT on 6 November (source of the giant arch No. 1) on the corona is not entirely clear, because one can propose two different interpretations of the SOLWIND data:

(1) There was no mass ejection associated with this flare, and the coronal condensation, left after the flare at 13 : 55 UT on 5 November, simply decayed and disappeared.

(2) There was a coronal mass ejection associated with the flare at 03 : 52 UT which swept away the condensation remaining after the earlier flare; the remnants of it could still be present in the SOLWIND image at 08 : 09 UT (Figure 2(d)), though their reality is marginal. A very extensive type IV burst and an accompanying type II burst seen at Culgoora (Robinson, 1986) also indicate the existence of a coronal transient. These observations (cf. Figure 2 in Robinson) show a moving type IV burst propagating eastwards between 03 : 56 and 05 : 30 UT with a speed of 670 km s^{-1} and a type II burst moving with a similar speed between 03 : 46 and 04 : 11 to the northeast. Thus, from the radio data, a (fast) mass ejection seems likely. Before discussing this event any further, let us look at the corresponding data revealed by the HELIOS spacecraft.

3. HELIOS-A Data

The HELIOS-A spacecraft had been idle until the morning hours of 6 November, 1980 when the photometers were switched on at the beginning of the spacecraft perihelion passage. The first useful image could be constructed from the 16-deg south photometer scans at 09 : 36 UT and showed excess material extending southwards slightly west of the Sun (Figure 3; cf. Jackson, 1985, for explanation of this method of imaging). Seven hours later, at 17 : 17 UT, a new mass ejection was added to it, directed towards the SSE. At that time HELIOS-A was 98 deg to the west of the Sun–Earth line at a distance of 0.60 AU from the Sun. Thus the ejections from AR 2779 were located for the HELIOS spacecraft on the opposite side of the Sun and the photometer looking 16 deg south could first see the mass ejection only after it reached a distance of at least 33 solar radii.

This second mass ejection decayed until 17 : 51 UT on 7 November. Another new ejection appeared to come from the Sun thereafter, its presence being first indicated at 10 : 44 UT on 8 November; it fully developed at 19 : 17 UT (cf. Figure 3).

The position of the ejection on the opposite side of the Sun implies that the excess material seen at 09 : 36 UT on 6 November could not originate in the flare at 03 : 52 UT,

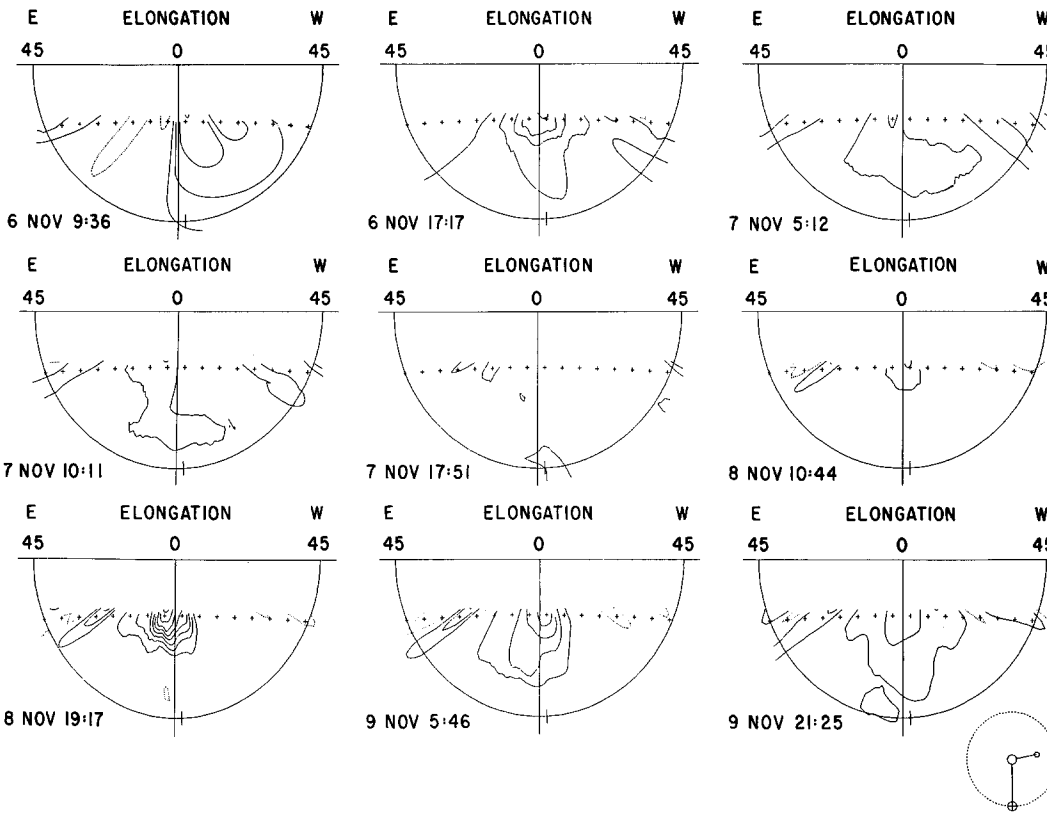

Fig. 3. HELIOS images of southward directed mass ejections on 6–9 November, 1980. Data are contoured in even-spaced levels of 25 × 10^{13} electrons cm^{-2} plus and minus from 15 × 10^{13} cm^{-2}. Negative contours are indicated by dotted lines. An existing ejection is present at the onset of observation at 09 : 36 UT on 6 November. New ejections can be recognized at 17 : 17 UT on 6 November (maximum density in the 16-deg photometers at that time) and at 10 : 44 UT on 8 November (maximum density at 19 : 17 UT on 8 November). A small display in the lower right-hand corner of the figure indicates the relative locations of the Earth, Sun, and spacecraft at the time of the last image.

because in that case the required speed would be unreasonably high. Even if the mass moved directly from the Sun to the photometer line-of-sight, i.e., 90 deg off the radial direction), the ejection speed would have to be greater than 1130 km s^{-1}. This flare at 03 : 52 UT, however, could be associated with the ejection seen at 17 : 17 UT, which requires an ejection speed of no more than 480 km s^{-1} if directed toward the HELIOS-A line-of-sight. In that case the first enhancement, seen by HELIOS at 09 : 36 UT, could be the aftermath of the ejection from the flare of 5 November (at 13 : 55 UT, with associated type II and IV radio bursts), propagating with a mean speed of at least 340 km s^{-1} if directed towards the HELIOS-A 16-deg photometer line-of-sight.

Thus the most likely conclusions based on HELIOS data are that:

(a) there was excess material observed when the HELIOS photometers were first turned on that was probably the aftermath of a mass ejection evidenced in metric radio data on the previous day;

(b) there was another mass ejection associated with the flare event at 03 : 52 UT on 6 November which propagated with a speed of at least 480 km s^{-1} and swept away the semi-stationary component of the first structure. This supports the interpretation (2) in the last paragraph of the preceding section.

As the other dynamic flares are concerned, HELIOS confirms the SOLWIND result that there were no mass ejections associated with them. If the dynamic flare at 15 : 26 UT on 6 November was associated with the HELIOS enhancement at 17 : 17 UT, the speed of propagation of the supposed mass ejection would be greater than 2900 km s^{-1}. The next HELIOS enhancement, first observed at 10 : 44 UT on 8 November, is most likely the onset of a filled-loop mass ejection seen in SOLWIND data directed southward at a height of 4 R_0 at 03 : 21 UT on the same date. No flare has been reported at that time at a suitable position, so that the most likely interpretation of this event is an eruption of a high-latitude filament.

If this mass ejection was identical with that seen by HELIOS, its speed would be 833 km s^{-1}. SOLWIND data give for it a speed of 755 km s^{-1}. The perspective view of this event from the SOLWIND coronagraph and HELIOS spacecraft confirm its high latitude. Using the technique described in Jackson *et al.* (1985), we find heliographic latitude solutions from 67 deg south to 85 deg south and longitudes that imply outward motion from the side of the Sun facing Earth. Thus, there is little doubt that the ejection observed by HELIOS at 10 : 44 UT on 8 November did not have its origin in AR 2779.

4. Summary

A series of dynamic flares in AR 2779 produced quasi-stationary giant coronal arches in the solar corona (Švestka, 1984) which lived for tens of hours hanging above the active region. Since some of the parent flares produced radio type II and IV bursts, it is likely that they were also associated with coronal mass ejections. We therefore have tried to clarify the problem how long-lived quasi-stationary structures and eruptive ejections can coexist in the same active region.

We have known for some time one of the sets of Hα footpoints of these arches (MS&B), while the second set of footpoints was ambiguous. Some supposed configurations (like in Figure 1(a)) implied that an eruptive instability along the neutral line (i.e., eruption of the active region filament) should disrupt these arches. However, as X-ray observations strongly indicate, at 15 UT on 6 November and at 05 UT on 7 November the pre-existing arch did not disrupt; it never disappeared but was simply revived in its brightness. Judging from the similarity of properties derived from X-ray observations (cf. Figures 3 and 6 in Švestka, 1984), the preceding arch, which was decaying prior to 15 UT on 6 November, also seemed to be a revived arch (Hick and Švestka, 1987).

This problem has become somewhat less severe after Kopp and Poletto (1988) modelled magnetic field lines rooted in the known set of footpoints and found the second set of footpoints rather far from the active region (Figure 1(b)). This configuration provides some degree of freedom for erupting structures along the $H_{\parallel} = 0$ line inside the

active region, but still the coexistence of stationary and eruptive structures remains peculiar. Therefore, we made a detailed analysis of the coronal mass ejections during this period.

Using data from both the SOLWIND coronagraph and HELIOS-A zodiacal light photometers we have arrived at the following conclusions.

The first flare of the series, at 13 : 55 UT on 5 November was associated with a mass ejection which was seen by HELIOS behind the Sun since the beginning of its perihelion operations at 09 : 36 UT on 6 November. SOLWIND imaged a slowly rising or stationary remnant of the coronal transient between 20 : 57 UT on 5 November and 00 : 47 UT on 6 November (Figures 2(b) and 2(c)). We have checked whether this perhaps might have been the high-corona top of the first giant arch over the active region, but this seems very unlikely, in particular because the following arches were not seen by SOLWIND. Apparently this was a different type of coronal condensation high in the solar corona which might have been left behind an earlier faster mass ejection.

Another mass ejection was associated with the following flare at 03 : 52 UT on 6 November which swept away the coronal condensation seen in Figures 2(b) and 2(c) and was seen by HELIOS at 17 : 17 UT the same day. This may imply that the arch No. 1 in Table I was not a revived arch, but that it formed only after the ejection was detached from the Sun. This contradicts the conclusion made by Hick and Švestka (1987) that the arch No. 1 was a revived arch. Thus one has to consider also the possibility that it was a revived arch and that the arch structure survived the mass ejection which blew out the coronal condensation at about 03 : 52 UT. In the configuration of Kopp and Poletto (Figure 1(b)) this would be possible if the ejection was so directed that it avoided the arch.

There is convincing evidence from both SOLWIND and HELIOS data that the following two flares which revived the arch (at 15 : 26 UT on 6 November and 04 : 58 UT on 7 November) were not associated with any mass ejection. The only southward directed mass ejection seen during the period after these events came from the southern polar region of the Sun and not from AR 2779.

Thus, the two dynamic flares which quite clearly did not disrupt the arch and caused only arch revivals (in temperature, density, and X-ray brightness) were without mass ejections. The flare that was responsible for the arch No. 1 was associated with a mass ejection (one can see it behind the Sun in the HELIOS image at 17 : 17 UT on 6 November in Figure 3). This arch was supposed to be a revival by Hick and Švestka, but we have no direct evidence that this really was the case. Thus either the rise of temperature maximum in the arch is not a feature associated solely with revived arches as Hick and Švestka have concluded; or, the mass ejection must have avoided the existing arch like in the case of the 21 May, 1980 flare, where however the mass ejection was highly anomalous (see McCabe *et al.*, 1986). The configuration of Figure 2(b) would make such an avoidance easier than in the 21 May case; on the other hand, the mass ejection at 03 : 52 UT seemed to have been a really powerful event according to its radio records (Robinson, 1986)). Stewart (in Švestka *et al.*, 1982b) describes the metric emission as 'one of the most extensive type IV radio bursts ever observed at Culgoora'.

Apparently, more events of giant arches and their associations with mass ejections are to be studied before one can better understand the connection between these two widely different coronal phenomena preceding and following dynamic flares.

Acknowledgements

Our thanks are due to Prof. Giannina Poletto for providing us with unpublished information about the inclination of the modelled potential fieldlines in the arch structure. Mr Hans Braun at Utrecht has helped in preparation of the figures. The work of B.V. Jackson and Z. Švestka was partly supported by the National Science Foundation Grant ATM-88–12409 with the University of California, San Diego.

References

Fárník, F., van Beek, H. F., and Švestka, Z.: 1986, *Solar Phys.* **104**, 321.
Hick, P. and Švestka, Z.: 1987, *Solar Phys.* **108**, 315.
Jackson, B. V.: 1985, *Solar Phys.* **100**, 563.
Jackson, B. V., Rompolt, B., and Švestka, Z.: 1988, *Solar Phys.* **115**, 327.
Jackson, B. V., Howard, R. A., Sheeley, N. R., Jr., Michels, D. J., Koomen, M. J., and Illing, R. M. E.: 1985, *J. Geophys. Res.* **90**, A6, 5075.
Karpen, J. T. and Howard, R. A.: 1987, *J. Geophys. Res.* **92**, 7227.
Kopp, R. A. and Poletto, G.: 1988, *Adv. Space Res. (Proc. COSPAR Helsinki)* (in press).
Martin, S. F., Švestka, Z., and Bhatnagar, A.: 1989, *Solar Phys.* (submitted) (Paper MS&B).
McCabe, M. K., Švestka, Z. F., Howard, R. A., Jackson, B. V., and Sheeley, N. R., Jr.: 1986, *Solar Phys.* **103**, 399.
Robinson, R. D.: 1986, *Solar Phys.* **104**, 33.
Sheeley, N. R., Stewart, R. T., Robinson, R. D., Howard, R. A., Koomen, M. J., and Michels, D. J.: 1984, *Astrophys. J.* **279**, 839.
Švestka, Z.: 1984, *Solar Phys.* **94**, 171.
Švestka, Z., Stewart, R., Hoyng, P., Van Tend, W., Acton, L. W., Gabriel, A. H., Rapley, C. G., and 8 co-authors: 1982a, *Solar Phys.* **75**, 305.
Švestka, Z., Dennis, B. R., Pick, M., Raoult, A., Rapley, C. G., Stewart, R. T., and Woodgate, B. E.: 1982b, *Solar Phys.* **80**, 143.
Van Beek, H. F., Hoyng, P., Lafleur, H., and Simnett, G. M.: 1980, *Solar Phys.* **65**, 39.